Journal of Power Sources 191 (2009) 489–494

Contents lists available at ScienceDirect

Journal of Power Sources

journal homepage: www.elsevier.com/locate/jpowsour

Effect of hydrophobic gas diffusion layers on the performance of the polymer exchange membrane fuel cell

Ching-Han Liu*, Tse-Hao Ko, Jin-Wei Shen, Su-I Chang, Shin-I Chang, Yuan-Kai Liao

Department of Materials Science and Engineering, Feng Chia University, No. 100 Wenhwa Rd., Seatwen, Taichung 40724, Taiwan

ARTICLE INFO

Article history:
Received 5 February 2009
Accepted 9 February 2009
Available online 20 February 2009

Keywords:
Fuel cell
Gas diffusion layer
Hydrophobic
Carbon fiber cloth
Carbonization

ABSTRACT

This study uses fuel cell gas diffusion layers (GDLs) fabricated in the laboratory from carbon fiber cloth with different concentrations of hydrophobic agents in proton exchange membrane fuel cells (PEMFCs), and investigates the relationship between the hydrophobic agent content of the carbon fiber cloth and fuel cell performance.

The paper examines the effect of hydrophobic agent content on GDL thickness, contact angle, air permeability, and surface and through-plane resistivity. Carbon fiber cloth is impregnated with hydrophobic agent concentrations of 0, 3, 5, 10, 30, and 50 wt%, and the resulting GDLs are subjected to performance tests. When the test piece area is 25 cm^2, the test temperature 80 °C, the gasket thickness 0.36 mm, and the hydrophobic agent content 5 wt%, a fuel cell using the GDL has a current density of 1430 mA cm^{-2} at 0.3 V.

1. Introduction

Because of their high efficiency, high power density, low operating temperature, and low noise, proton exchange membrane fuel cells (PEMFCs) are thought to be superior to other fuel cell systems in vehicle applications [1–4]. Although gas diffusion layers (GDLs) comprise only one part of a fuel cell, differences in the concentration of hydrophobic agent in the GDL can affect the performance of the fuel cell as a whole. Carbon fiber fabric or carbon fiber papers are currently the most common materials used to make GDLs. Because carbon possesses the advantages of high conductivity and corrosion resistance, it is very well suited to the special environment inside a fuel cell. GDLs are usually produced by subjecting oxidized carbon fiber felt or oxidized carbon fiber cloth to high-temperature carbonization in a carbonizing furnace. This alters the structure of the material and increases conductivity, yielding processed carbon fiber paper or carbon fiber cloth [5]. Research on carbon fiber has shown that graphitization temperature has a significant effect on the microstructure and properties of the material, and conductivity increases with graphitization temperature [6]. We choose a carbonization temperature of 1400 °C in this paper.

A GDL composed of gas diffusion backing (GDB, carbon fiber paper or carbon cloth) and a micro-porous layer (MPL) not only serves as a pathway for the diffusion of fuel to the electrode, but also as a conduit for the removal of byproduct water from the electrode. A GDL is typically treated by partial coating with a hydrophobic polymer to prevent flooding of the electrode by water. The hydrophobic agent used is usually polytetrafluoroethylene (PTFE) or fluorinated ethylene propylene (FEP) [7–9]. Various types of carbon powder (such as Volcan XC-72 or Shawinigan Acetylene Black (SAB)) and graphite (such as MogulL or Asbury 850) were added during MPL fabrication in prior studies [10–14]; although it was found that graphite yields good conductivity, the aggregation of graphite leads to the presence of irregularly distributed large voids, which are detrimental to the passage of gas and water. Some early studies [15–17] considered the effects of GDL electrical resistance, and showed that, under certain conditions, the resistance of a GDL is sufficient to alter the current density distribution of the gas channels and bulk areas. No carbon was added during MPL fabrication in this study, but attention was paid to the hydrophobic agent concentration and its relationship with fuel cell performance. The concentration of the hydrophobic agent, FEP, ranged from 0 to 50 wt%. The goal of this study was to determine the effect of various hydrophobic agent concentrations on the performance of a PEMFC system.

This study focused on GDL fabrication technology, and sought to boost fuel cell performance through improved GDLs. We examine the relationship between fuel cell performance and the hydrophobic agent content of the GDL's carbon fiber cloth, and investigate the effect of hydrophobic agent content on thickness, contact angle, air permeability, and surface and through-plane resistivity.

* Corresponding author. Tel.: +886 4 24517250x5303; fax: +886 4 24518401.
E-mail address: wowbabytw@gmail.com (C.-H. Liu).

0378-7753/$ – see front matter © 2009 Elsevier B.V. All rights reserved.
doi:10.1016/j.jpowsour.2009.02.017

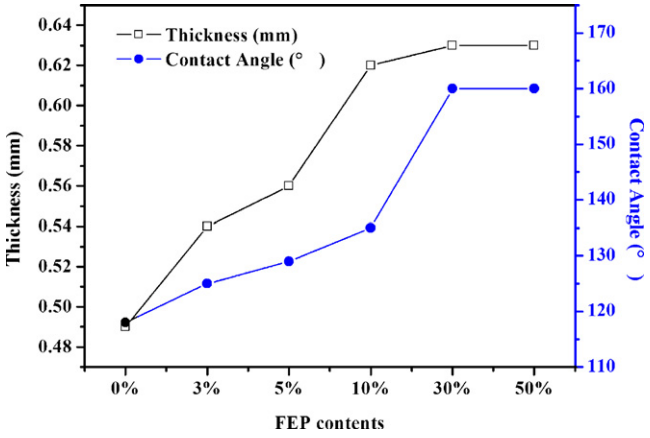

Fig. 1. Relationship between thickness and contact angle of carbon fiber cloth pieces impregnated with different FEP concentrations: (□) thickness and (●) contact angle.

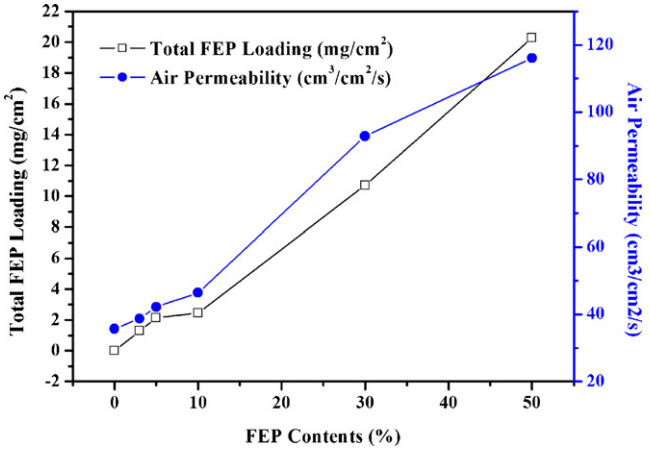

Fig. 3. GDL air permeability and total FEP loading for GDLs produced using different FEP concentrations: (□) total FEP loading and (●) air permeability.

2. Experiment

A GDL consists of a GDB and a micro-porous layer MPL. The GDB is usually made from carbon fiber paper or carbon fiber cloth. The GDBs used in this study were fabricated from carbon fiber in accordance with Taiwan patent I296449. Two pieces of carbon fiber cloth 5 cm × 5 cm in size were used as the anode and cathode of each fuel cell during GDL testing. The temperature of the carbonization furnace was set at 1400 °C. We employed 0%, 3%, 5%, 10%, 30%, and 50% FEP solutions (as an example, the 10% FEP solution was prepared by diluting 10 mL Dupont FEP 121A solution in 90 mL deionized water and stirring for 5 min at room temperature) to obtain the different hydrophobic agent concentrations. The impregnated GDBs were baked dry at 70 °C for 15 min, baked at 240 °C for 30 min, and sintered at 350 °C for 30 min.

The thickness, contact angle, air permeability, and surface and through-plane resistivity of each piece were measured. A Teclock SM-114 thickness tester was used to measure the thickness of the carbon cloth, and thickness was determined from the average of measurements taken at five random points. A Gurley Model 4320 meter was used to measure air permeability and testing and analysis of air permeability was performed in accordance with Model 4110 regulations. A Loresta GP MCP-T600 meter was used to measure surface resistivity and testing and analysis of surface resistivity was performed in accordance with JIS K 7194 regulations. Through-plane resistivity was measured via the two-point method, using copper plates 10 mm apart. Measurements were made at a minimum of five points on each GDL at different pressures. Surface hydrophobicity was determined by measurement of contact angle. The measurements were carried out with a contact angle meter (FTA 125, First Ten Angstroms) at room temperature. A cold field emission scanning electron microscope was used to analyze the surfaces and cross-sections of the GDLs.

Preparing the carbon cloth for use as fuel cell GDLs entailed cutting the cloth into 5 cm × 5 cm pieces and then forming three-layer membrane electrode assemblies (MEAs) with catalyst-coated membrane (CCM) from Dupont™ (type NRE-211). This study focused exclusively on the effect of hydrophobic agent concentration on the GDL, and we applied a hydrophobic layer on carbon cloth. We did not bond the CCM and carbon cloth together by hot-pressing, but only used 40 kgf cm^{-1} torsion to ensure close contact between the layers. The MEA was placed in a fuel cell testing module. The activated area was 25 cm^2, and the bipolar plates were gate-type grooved graphite plates made of highly compacted graphite. Gas flow at the anode (H_2) was 500 cm^3 min^{-1}, and gas flow at the cathode (O_2) was also 500 cm min^{-1} (both gases had a relative humidity of 95%); the temperatures of the anode and cathode were 40 and 80 °C respectively. All single cell operations were performed without external pressurization, and used humidified pure hydrogen and pure oxygen. The gas inlet pressure was

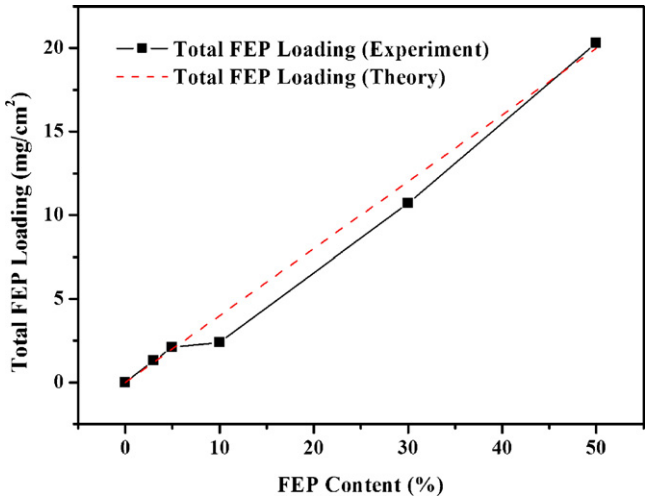

Fig. 2. Changes in the loading of carbon fiber cloth pieces impregnated with different FEP concentrations.

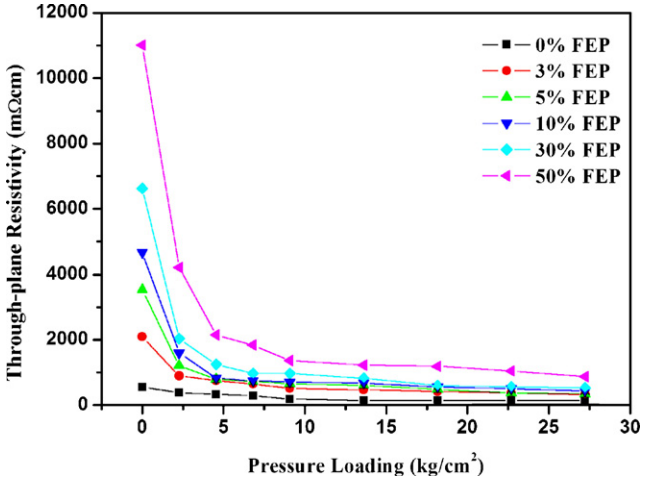

Fig. 4. Changes in through-plane resistivity at different pressures of GDLs produced using different FEP concentrations.

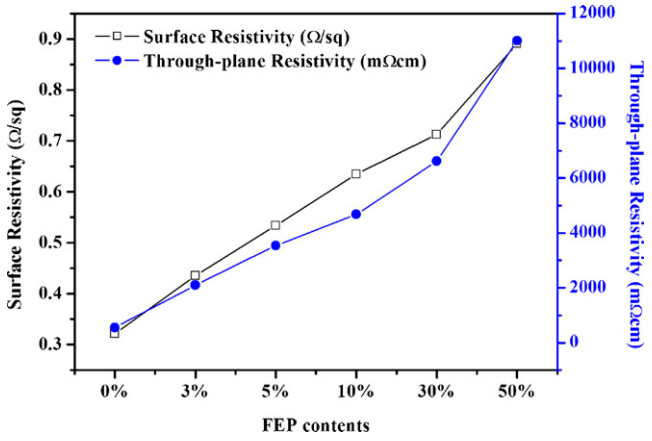

Fig. 5. Surface resistivity and through-plane resistivity curves for GDLs produced using different FEP concentrations: (□) surface resistivity and (●) through-plane resistivity.

1 kg cm^{-2}, and cell temperature during testing was set at 40 and 80 °C. The gasket thickness was 0.36 mm.

3. Results and discussion

Fig. 1 shows the relationship between thickness and contact angle for carbon fiber cloth pieces impregnated with different FEP concentrations. In this figure, the □ curve is the thickness curve for GDL impregnated with different concentrations of FEP, and the ● curve is the contact angle curve for GDLs impregnated with different concentrations of FEP. It can be seen from this chart that the thickness raises as the FEP concentration of the solution increases. When the FEP content was 0%, the GDLs had a thickness of 0.49 mm. When FEP was increased to 10%, the thickness of the GDL rose by 26.5% to 0.62 mm. When FEP was increased to 50%, the thickness of the GDL rose to 0.63 mm. This indicates that the thickness of the carbon fiber cloth does not increase significantly when FEP concentration is greater than 10%. It also suggests that, when the FEP concentration is relatively low, most of the FEP is deposited on the surface of the carbon fiber cloth. With regard to contact angle, in the case of carbon fiber cloth with no FEP, the GDL had a contact angle of 118°, which indicates that the GDL is already quite hydrophobic. When the FEP concentration was increased to 10%, the contact angle of the GDL increased to 135°. The contact angle was >160° when the FEP concentration was 30% or above. The fact that the contact angle

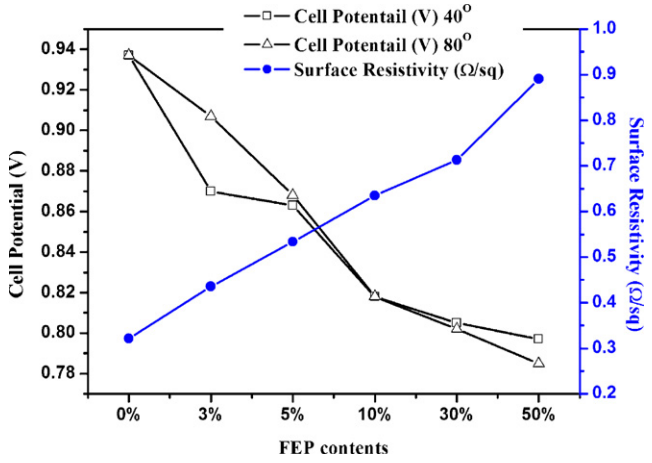

Fig. 6. Relationship between OCP and FEP concentration and surface resistivity at temperatures of 40 and 80 °C when a 0.36-mm gasket was used: (□) 40 °C, (△) 80 °C, (●) surface resistivity.

increases with FEP concentration indicates that the hydrophobicity of carbon fiber cloth increases as its FEP content rises. It is evident that contact angle has a very significant correlation with concentration, and has an especially strong connection with FEP deposited on the surface of the GDB.

Fig. 2 shows changes in the loading of carbon fiber cloth impregnated with different FEP concentrations. The experimental data reveals that each 1% increase in FEP causes the weight to increase by roughly 0.4 mg cm^{-2}. Total FEP loading increased with FEP concentration. The total loading of sample GDL was 1.3 mg cm^{-2} when the FEP concentration was 3%, 2.4 mg cm^{-2} when the concentration was 10%, and 20.3 mg cm^{-2} when the concentration was 50%. Since, as shown in Fig. 1, the thickness and contact angle do not increase significantly after FEP reaches 30%, we can infer that while high FEP concentrations will result in the carbon fiber cloth with a greater FEP loading, most of the FEP will subsequently be deposited inside the cloth.

Fig. 3 shows the GDL air permeability and total FEP loading curves for GDLs produced using different FEP concentrations. In this figure, the □ curve is the total FEP loading curve for GDLs produced using different FEP concentrations, and the ● curve is the air permeability curve for GDLs produced using different FEP concentrations. It can be seen from this figure that the total FEP loading of the GDL raises steadily as the FEP concentration increases. In addition, air permeability also exhibits a clear rising trend as the FEP concentration increases. The air permeability of a GDL pro-

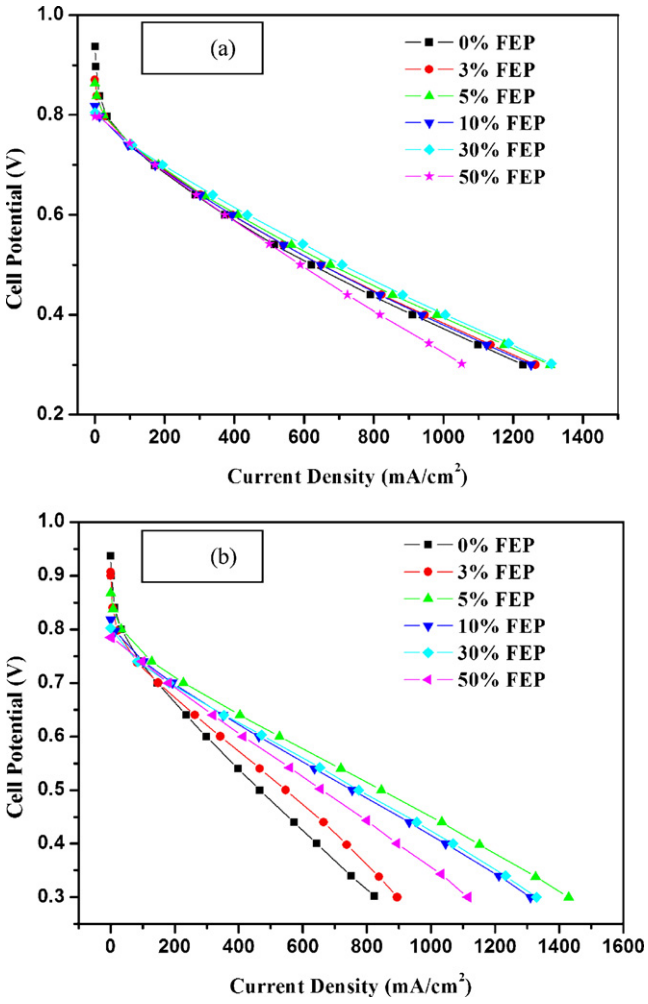

Fig. 7. Fuel cell polarization curves for GDLs prepared using carbon fiber cloth impregnated with different FEP concentrations: (a) 40 °C and (b) 80 °C.

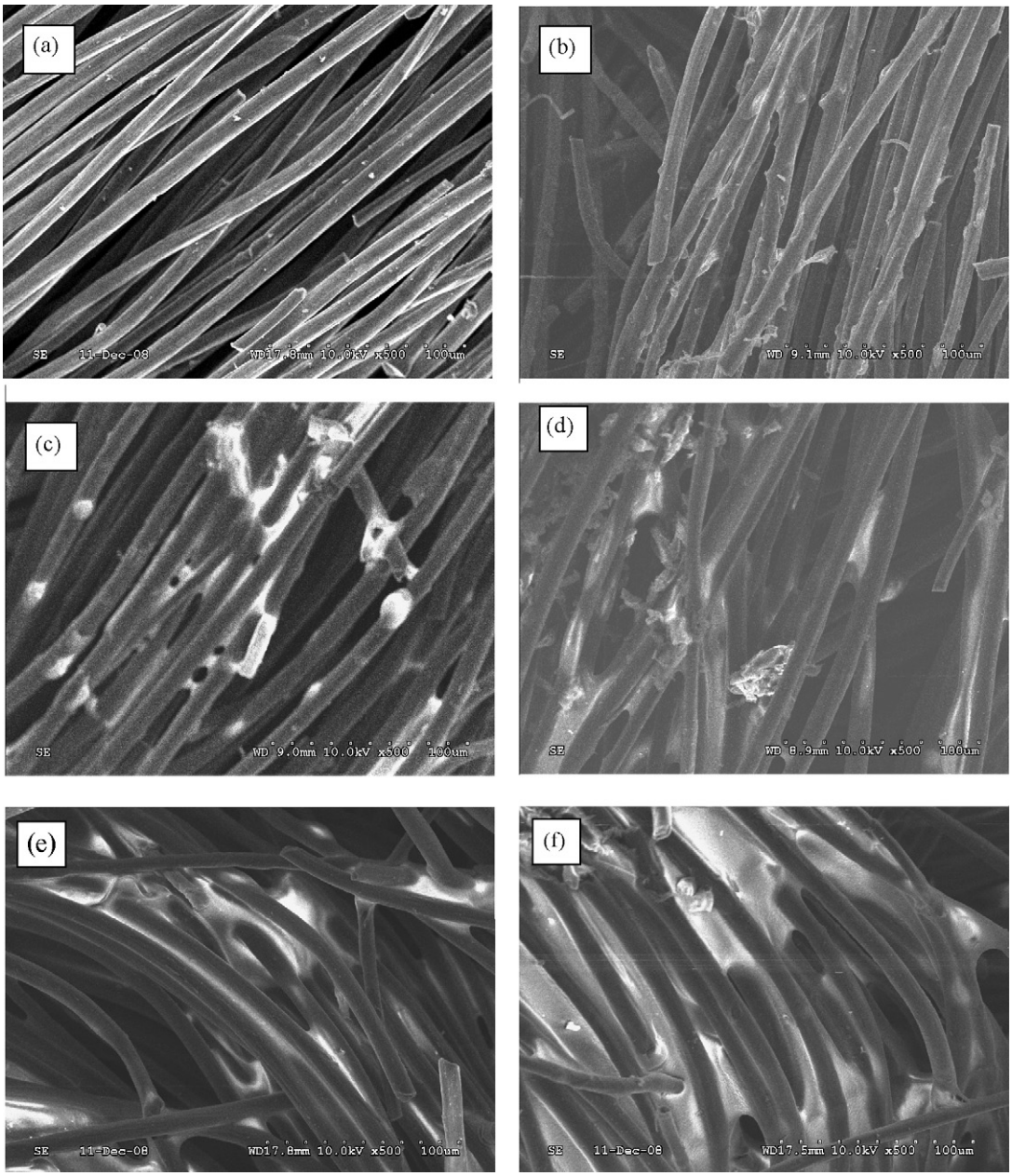

Fig. 8. SEM micrographs of the surface of carbon fiber cloth containing different FEP concentrations: (a) 0%, (b) 3%, (c) 5%, (d) 10%, (e) 30%, and (f) 50%.

duced using 0% FEP was 35 $cm^3\ cm^{-2}\ s^{-1}$, while that of a GDL produced using 50% FEP was 116 $cm^3\ cm^{-2}\ s^{-1}$. This is an increase of approximately 231%.

Fig. 4 shows the through-plane resistivity at different pressures of GDLs produced using different FEP concentrations. Through-plane resistivity was measured when the test pieces were subjected to pressures of 0, 5, 10, 15, 20, 30, 40, 50, and 60 lbs (0, 2, 4.5, 7, 9, 14, 18, 23 and 27 $kg\,cm^{-2}$). It can be seen that through-plane resistivity decreased as the pressure increased. The through-plane resistivity of GDLs with 0% FEP was 550 mΩ when there was no applied pressure. The through-plane resistivity increased with FEP concentration, rising to 4700 mΩ when FEP concentration was 10% and 11,000 mΩ when FEP concentration was 50%. This trend occurs because FEP is non-conducting, and increasing the FEP concentration in a GDL will therefore decrease conductivity and increase through-plane resistivity. Through-plane resistivity decreases, however, when pressure is increased. Taking a GDL with 0% FEP as an example, compared with a pressure of 0 lbs, through-plane resistivity fell 47% to 290 mΩ at a pressure of 15 lbs (7 $kg\,cm^{-2}$), and fell even further to 150 mΩ at a pressure of 30 lbs (14 $kg\,cm^{-2}$), which was a decrease of 72% compared with no applied pressure. It can be seen that through-plane resistivity falls steadily as the pressure increases. This is because increasing the pressure causes the fibers of carbon fiber cloth to bind together more tightly, which provides more pathways for electron transmission, and thereby increases conductivity and reduces resistivity. It can also be seen from this figure that, after the pressure reaches a limit, a further increase in pressure will not continue to improve conductivity. This is because the compression of the GDL has reached a maximum; since the material will not continue to compress, there will no longer be new pathways or contact between fibers to increase the conductivity. As a result, the through-plane resistivity will not continue to fall after the pressure reaches a limiting value, but will instead remain roughly constant.

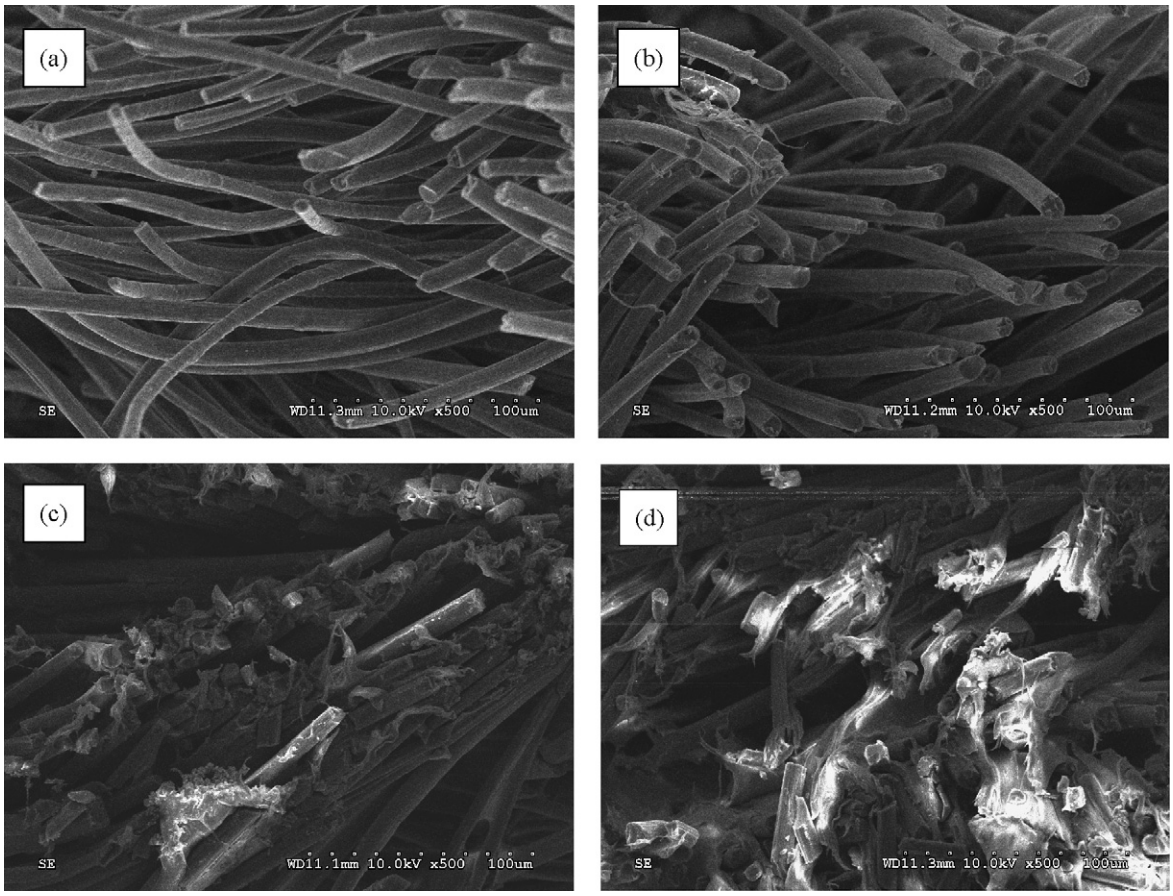

Fig. 9. SEM micrographs of the cross-section of carbon fiber cloth containing different FEP concentrations: (a) 0%, (b) 10%, (c) 30%, and (d) 50%.

Fig. 5 shows the surface resistivity and through-plane resistivity curves for GDLs produced using different FEP concentrations. In this figure, the □ curve is the surface resistivity curve for GDLs produced using different FEP concentrations, and the ● curve is the through-plane resistivity curve for GDLs produced using different FEP concentrations. Here the through-plane resistivity is measured with no applied pressure. Surface resistivity and through-plane resistivity are the two main ways of measuring the conductivity of a GDL. The surface resistivity measures conduction along the surface of the GDL, and through-plane resistivity measures conduction perpendicular to the surface. This figure reveals that both surface resistivity and through-plane resistivity rise, and conductivity falls, with increasing FEP concentration. The surface resistivity increases by 65% from 0.32 $\Omega\,sq^{-1}$ for 0% FEP to 0.53 $\Omega\,sq^{-1}$ for 5% FEP, and increases further to 0.89 $\Omega\,sq^{-1}$ for 50% FEP. This trend occurs because FEP is non-conducting, and increasing the FEP concentration in a GDL will cause surface deposition to increase and surface conductivity to decrease. When there is no applied pressure, through-plane resistivity will increase, and conductivity decrease, with FEP concentration. This is because, apart from surface deposition, FEP is also deposited throughout the cloth, where it causes through-plane resistivity to increase.

Fig. 6 shows the relationship between open circuit potential (OCP), FEP concentration, and surface resistivity at temperatures of 40 and 80 °C when a 0.36-mm gasket was used. In this figure, the □ curve is the OCP curve for GDLs at 40 °C, △ is the OCP curve for GDLs at 80 °C, and ● is the GDL surface resistivity curve. It can be seen from Fig. 6 that, when the temperature was 40 °C, the OCP of GDLs prepared with 0% FEP concentration was 0.94 V, the OCP of GDLs prepared with 5% FEP concentration was 0.86 V, and the OCP of GDLs prepared with 50% FEP concentration was 0.79 V. It can be discovered that the greater the surface resistivity of the GDL, the lower the OCP, and the worse the fuel cell performance. It is also clear from Fig. 5 that when surface resistivity and through-plane resistivity are mutually dependent, the greater the FEP concentration, the worse the OCP. The GDL-related factor in this study influencing fuel cell OCP was the resistance of the GDL. Because increasingly FEP concentration causes a GDL's surface and through-plane resistivity to increase, this also causes the overall cell internal resistance to increase, which will result in a lower OCP. As a consequence, increasing FEP concentration will result in a decreasing OCP.

When GDLs prepared using carbon fiber cloth impregnated with different FEP concentration were used to assemble single-cell batteries with 0.36 mm gaskets, the polarization curves at 40 °C were as shown in Fig. 7(a). It can be seen that GDLs prepared using a 0% FEP concentration and GDLs prepared using 30% FEP yielded roughly equally good cell performance; when the loading was 0.3 V, the current densities of these cells were in the range of 1200–1300 mA cm^{-2}. When GDLs prepared using a 50% FEP concentration were tested with a loading of 0.3 V, the current density was 1000 mA cm^{-2}. The polarization curves at 80 °C are as shown in Fig. 7(b). Here GDLs prepared using a 30% FEP concentration yielded relatively optimal cell performance, and had a current density of approximately 1400 mA cm^{-2} when the loading was 0.3 V. In the case of GDLs with 50% FEP, the current density was approximately 1100 mA cm^{-2} when the loading was 0.3 V. GDLs with 0% FEP had a current density of roughly 800 mA cm^{-2} when the loading was 0.3 V. Because an operating temperature of 40 °C is relatively low, water management is easy, and there is little tendency for water accumulation to degrade cell performance. Current density at a loading of 0.3 V consequently does not vary significantly for FEP concentrations in the range of 0–30%. In the case of GDLs with 50%

FEP, however, the high resistivity indicates poor conduction, which resulted in the worst cell performance. When the reaction temperature was 80 °C, the relatively high operating temperature led to more significant flooding problems, which allowed the hydrophobic FEP to play a more important role. It can be seen that a GDL prepared using a 5% FEP concentration yields excellent cell performance at this temperature. While cell performance declined for higher FEP concentrations, as in the case of GDLs with 50% FEP, due to the high resistance of the GDL, cell performance was also poor for 0% FEP GDLs due to flooding problems.

Use of a SEM microscope to examine the GDLs revealed that the method used in this study induced the FEP to effectively enter the carbon raw material, where it adhered on and between the fibers after sintering. Carbon fiber cloth without any added FEP is as shown in Fig. 8(a) and Fig. 9(a). The carbon fiber cloth begins to display some FEP deposition when the FEP concentration rises to 3%, as shown in Fig. 8(b). In Fig. 8(d) and Fig. 9(b), relatively evident FEP deposition can be seen when the FEP concentration is 10%. Apart from evident surface FEP deposition, internal FEP deposition also occurs when the FEP is increased to 30% and 50%, as shown respectively in Fig. 8(e) and (f) and Fig. 9(c) and (d). While the FEP is first deposited on the surface when FEP concentration is low, internal deposition also occurs when the concentration is high. As the FEP concentration increases, the resistance of the GDL will also increase, which leads to poor performance. On the other hand, when a GDL has received no hydrophobic treatment, flooding and poor performance tend to occur at high operating temperatures.

4. Conclusions

Carbon fiber cloth pieces were soaked in solutions variously containing 0%, 3%, 5%, 10%, 30%, and 50% FEP to prepare gas diffusion layers for use as fuel cell electrodes. The GDL thickness was 0.49 mm when the FEP concentration was 0%, 0.62 mm when the concentration was 10%, and 0.63 mm when the concentration was 50%. GDL thickness thus increases with FEP concentration. Air permeability also increases with FEP concentration. The air permeability of GDLs with 0% FEP was 35 $cm^3\ cm^{-2}\ s^{-1}$, while that of GDLs with 50% FEP was 116 $cm^3\ cm^{-2}\ s^{-1}$. Surface resistivity and through-plane resistivity likewise increased with FEP concentration: when there was no applied pressure, GDLs with 0% FEP had through-plane resistivity of 550 mΩ and surface resistivity of 0.32 $\Omega\ sq^{-1}$, while GDLs with 50% FEP had through-plane resistivity of 11,000 mΩ and surface resistivity of 0.89 $\Omega\ sq^{-1}$. As far as fuel cell performance was concerned, when a 0.36 mm gasket was used, a GDL produced using a 5% FEP concentration yielded excellent performance at an operating temperature of 80 °C: current density was 1400 mA cm^{-2} with a loading of 0.3 V.

Acknowledgements

The authors wish to thank the Ministry of Economic Affairs, R.O.C. (97-EC-17-A-08-S1-099) and National Science Council, R.O.C. (NSC97-2221-E-035-007-MY2) for financial support.

References

[1] S.D. Fritts, R. Gopal, J. Electrochem. Soc. 140 (1993) 3347.
[2] A. Parthasarathy, S. Srinivasan, J. Appleby, C.R. Martin, J. Electroanal. Chem. 339 (1992) 101.
[3] R.A. Lemons, J. Power Sources 29 (1990) 251.
[4] G. Hoogers, Fuel Cell Technology Handbook, CRC Press LLC, 2002.
[5] M.V. Williams, E. Begg, L. Bonville, H. Russell Kunz, J.M. Fenton, J. Electrochem. Soc. 8 (2004) 1173–1180.
[6] M.Z. Wang, New Carbon Mater. 13 (1998) 79.
[7] C. Lim, C.Y. Wang, Electrochim. Acta 49 (2004) 4149–4156.
[8] J. Moreira, A.L. Ocampo, P.J. Sebastian, M.A. Smit, M.D. Salazar, P. del Angel, J.A. Montoya, R. Peĭrez, L. Martiĭnez, J. Int. Hydrogen Energy 28 (2003) 625–627.
[9] S. Park, J.W. Lee, B.N. Popov, J. Power Sources 163 (2006) 357–363.
[10] E. Antolini, R.P. Passos, E.A. Ticianelli, J. Power Sources 109 (2002) 477–482.
[11] G.G. Park, Y.J. Sohn, S.D. Yim, T.H. Yang, Y.G. Yoon, W.Y. Lee, K. Eguchi, C.S. Kim, J. Power Sources 163 (2006) 113–118.
[12] X.L. Wang, H.M. Zhang, J.L. Zhang, H.F. Xu, X.B. Zhu, J.A. Chen, B.L. Yi, J. Power Sources 162 (2006) 474–479.
[13] X.L. Wang, H.M. Zhang, J.L. Zhang, H.F. Xu, Z.Q. Tian, J. Chen, H.X. Zhong, Y.M. Liang, B.L. Yi, Electrochim. Acta 51 (2006) 4909–4915.
[14] L.R. Jordan, A.K. Shukla, T. Behrsing, N.R. Avery, B.C. Muddle, M. Forsyth, J. Power Sources 86 (2000) 250–254.
[15] H. Meng, C.Y. Wang, J. Electrochem. Soc. 151 (2004) 358–367.
[16] B.R. Sivertsen, N.J. Djilali, Power Sources 141 (2005) 65–78.
[17] T. Zhou, H.J. Liu, Power Sources 161 (2006) 444–453.